

The Role of Docosahexaenoic Acid in Retinal Function

Brett G. Jeffrey^{a,c}, Harrison S. Weisinger^{b,d}, Martha Neuringer^{c,*}, and Drake C. Mitchell^d

^aDepartment of Paediatrics and Child Health, Flinders Medical Centre, The Flinders University of South Australia, Bedford Park (Adelaide), South Australia 5042, Australia, ^bDepartment of Food Science, Royal Melbourne Institute of Technology University, Melbourne, Victoria 3000, Australia, ^cOregon Regional Primate Research Center, Oregon Health and Science University, Portland, Oregon, 97201, and ^dLaboratory of Membrane Biochemistry and Biophysics, National Institute on Alcohol Abuse and Alcoholism, National Institutes of Health, Bethesda, Maryland 20892

ABSTRACT: An important role for docosahexaenoic acid (DHA) within the retina is suggested by its high levels and active conservation in this tissue. Animals raised on n-3-deficient diets have large reductions in retinal DHA levels that are associated with altered retinal function as assessed by the electroretinogram (ERG). Despite two decades of research in this field, little is known about the mechanisms underlying altered retinal function in n-3-deficient animals. The focus of this review is on recent research that has sought to elucidate the role of DHA in retinal function, particularly within the rod photoreceptor outer segments where DHA is found at its highest concentration. An overview is also given of human infant studies that have examined whether a neonatal dietary supply of DHA is required for the normal development of retinal function.

Paper no. L8652 in *Lipids* 36, 859–871 (September 2001).

Docosahexaenoic acid (DHA, 22:6n-3) is found in very high concentration in the retina (1,2). DHA may be obtained directly from the diet or synthesized from one of its n-3 precursors (3). The retina possesses an efficient conservation and recycling mechanism that helps preserve retinal DHA concentrations even during prolonged periods of low n-3 dietary intake (4–6). The high concentration of DHA in the retina and existence of the conservation and recycling mechanisms suggest that DHA may be important to retinal function. The growing body of evidence to suggest that DHA performs several important roles within the retina is the subject of this review. We have chosen to focus on recent research that has provided new information regarding the role of DHA in the retina, particularly within the photoreceptors. Key results from early studies that have contributed to our understanding of the role of DHA in the retina are also discussed. A comprehensive review of earlier studies in this field was published previously (7).

A major portion of this review is dedicated to animal studies that have investigated the effect of large reductions in retinal DHA levels on retinal function. An overview is also given

*To whom correspondence should be addressed at Oregon Regional Primate Research Center, Oregon Health and Science University, 505 N.W. 185th Ave., Beaverton, OR 97006.
E-mail: neuringe@ohsu.edu

Abbreviations: AA, arachidonic acid; ALA, α -linolenic acid; DHA, docosahexaenoic acid; E, cGMP phosphodiesterase; EPA, eicosapentaenoic acid; ERG, electroretinogram; IPR, isolated probe response; IRBP, interphotoreceptor retinal binding proteins; ISI, interstimulus interval; LC-PUFA, long-chain polyunsaturated fatty acids; PE, phosphatidylethanolamine; ROS, rod outer segment; RPE, retinal pigment epithelium.

of studies with human infants that have sought to determine whether a supply of preformed DHA is required in the diet of human infants to achieve optimal retinal function. A description of the basic structure and physiology of the retina and how its function may be assessed with the electroretinogram (ERG) will preface the review of the human and animal studies.

THE RETINA

The following sections provide a brief overview of basic retinal structure and physiology; more detailed information on these subjects may be found elsewhere (for review, see Refs. 8–10). The process of vision begins with light being focused through the cornea and lens onto the retina. The retina contains the cells responsible for light capture and transduction, the rod and cone photoreceptors. The rod system has high sensitivity at low light levels to provide animals with “night vision,” but does not provide color vision or high spatial resolution. The retinas of nocturnal mammals such as rats are rod dominant and have few cones. Cones provide the basis for color vision and the ability to see over a wide range of light intensities in daylight. Higher primates, including humans, apes and old world monkeys, have three classes of cones that respond optimally to either long, medium, or short wavelengths (i.e., red, green, or blue) (11). Cones are tightly packed within the fovea to provide the basis for high visual acuity.

Photoreceptor cells contain two distinct compartments, the inner and outer segments (Fig. 1). The inner segments contain the components necessary for cell metabolism, whereas the outer segments contain the photopigments that absorb photons of light. The rod outer segments (ROS) contain thousands of vertically stacked free-floating disks that are rich in DHA and the photopigment rhodopsin (Fig. 1). The cone photoreceptors also contain disks within the outer segment, but they are not free floating and remain contiguous with the outer plasma membrane.

In the dark, a continuous current flows into the rod photoreceptor outer segments through cation channels kept open by a high cytosolic concentration of cGMP (see Fig. 2). After photon capture, rhodopsin rapidly undergoes a conformational change to form metarhodopsin II (R*), the activated form of rhodopsin. R* activates the trimeric G protein, transducin, by catalyzing the exchange of GDP for GTP, which binds to the α subunit of transducin (Fig. 2). The activated

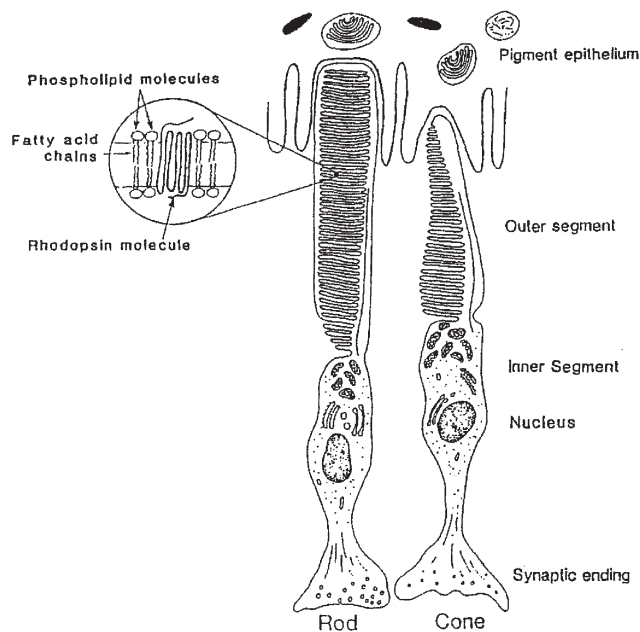


FIG. 1. Rods contain thousands of vertically stacked free-floating disks that are rich in docosahexaenoic acid (DHA) and the photopigment, rhodopsin. The cone photoreceptors also contain disks within the outer segment, but they are not free floating and remain contiguous with the outer membrane. Each cone photoreceptor contains one of three photopigments that respond optimally to short, medium or long (red, green or blue) wavelength light. The inner segments contain the components necessary for cell metabolism. The pigment epithelium has several important roles including regulation of the exchange of nutrients and by-products between the photoreceptors and the choroidal blood supply. Inset: The photopigments are surrounded by the DHA-rich phospholipids. Reproduced with permission from Reference 7.

transducin ($G\alpha^*$) binds to the tetrameric cGMP phosphodiesterase (E), thus removing the influence of one of its inhibitory γ subunits. The activated E (E^*) hydrolyzes cGMP to GMP. The resulting fall in cytosolic cGMP after rhodopsin activation closes cation channels causing the photoreceptor to hyperpolarize. The phototransduction cascade has a high gain, so the activation of a single rhodopsin molecule results in the hydrolysis of some 10^5 cGMP molecules (12).

In the dark, photoreceptors continually release the neurotransmitter glutamate into their synaptic junctions with the bipolar and horizontal cells. Light-induced hyperpolarization of the photoreceptors causes a graded reduction in the release of glutamate, which in turn causes the bipolar cells to either depolarize (ON-bipolars) or hyperpolarize (OFF-bipolars).

THE ERG AS A MEASURE OF RETINAL FUNCTION

The ERG is a record of the voltage change that occurs across the retina in response to a brief flash of light (for reviews, see Refs. 10,13). The ERG may be recorded using a wide variety of electrodes, but a contact lens electrode placed on the cornea provides the largest and most stable response (14). The

following section gives a brief overview of the ERG with particular reference to the components most commonly recorded in studies that have assessed the role of DHA in retinal function. A typical ERG and its characteristic parameters are shown in Figure 3.

Origin of the ERG. The leading edge of the ERG a-wave recorded to a bright saturating flash, i.e., one that closes all cation channels, reflects the hyperpolarization of the massed photoreceptor response (15,16). The rod-dominated ERG b-wave recorded in the dark reflects depolarization of the rod bipolar cells (17,18). The cone-dominated ERG b-wave recorded with a bright background is shaped by both ON and OFF bipolar cells and horizontal cells (19). The oscillatory potentials are high-frequency oscillations superimposed upon the b-wave (Fig. 3), and are thought to originate from different levels within the proximal retina, including the amacrine, interplexiform, and ganglion cells (20).

Factors affecting ERG morphology. One important determinant of ERG amplitudes and implicit times is the retinal illuminance produced by the flash. Retinal illuminance refers to the number of photons arriving at the retina measured in trolands (Td) (21). Retinal illuminance takes into account not only the intensity and spectral content (color) of the flash but also a number of other factors, including dark adaptation, the length of the eye, and the size of the pupil (21). It has been estimated for dark-adapted humans that a troland of light induces, on average, 8.6 photoisomerizations per rod (22). For the average human rod with 70 million rhodopsin molecules (9), a flash that produces a retinal illuminance of 1.0 log scotopic troland-seconds (scot-Td-sec) will therefore bleach ~0.0001% of the available rhodopsin.

Another important determinant of ERG morphology is the background luminance. Scotopic ERG (rod dominant) are recorded in the dark, whereas photopic ERG (a measure of the massed cone response) are recorded against a background light sufficient to saturate the rods. Photopic ERG are typically smaller and faster than scotopic ERG (23).

Conventional analysis of the ERG. The “conventional” method of ERG assessment involves measurement of ERG b-wave amplitude over a range of flash intensities (Fig. 4). The change in amplitude with flash intensity may be described in terms of the Naka-Rushton function (Fig. 5), an adaptation of the Michaelis-Menten equation (24,25):

$$V/V_{\max} = I^n / (I^n + K^n) \quad [1]$$

where V is the amplitude (μV), I is the flash intensity, n is the slope of the curve, V_{\max} is the maximum amplitude (μV), and K is the intensity that elicits half-maximal response. V_{\max} has been interpreted as an index of both the number of rods responding and the gain ($\mu\text{V}/\text{quantum captured}$) for each b-wave generator (26). The parameter K has been interpreted as an index of retinal sensitivity that represents quantal capture (26). Rod threshold, defined as the flash intensity at which an ERG b-wave is just detectable, may also be determined from the Naka-Rushton equation (27).

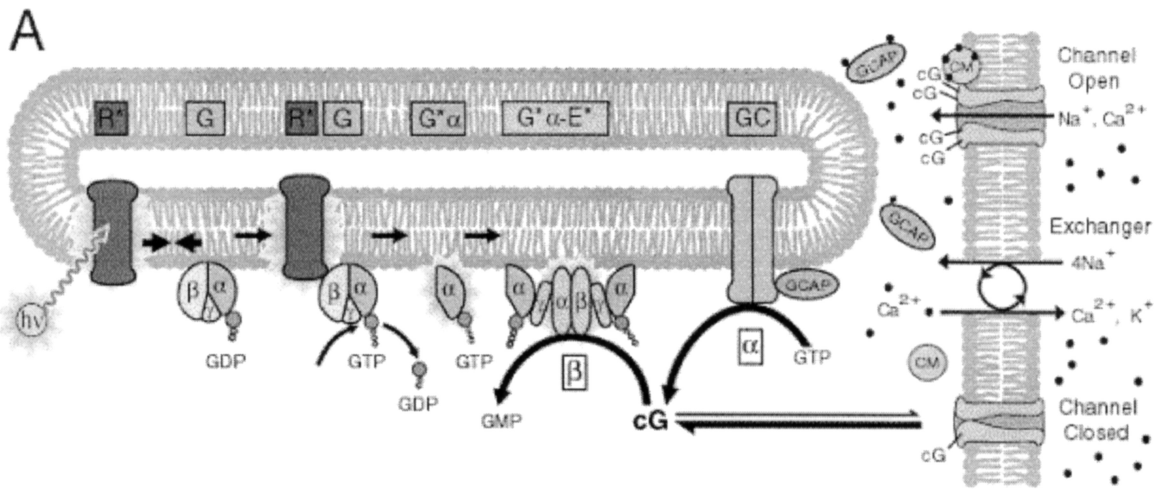


FIG. 2. Upon capture of a photon of light (hv), rhodopsin is activated (R*). R* activates the G protein by catalyzing the exchange of GDP for GTP. Upon activation, the G protein separates into two parts; one is the isolated subunit to which GTP is now attached (G*α). G*α binds to cyclic guanosine monophosphate phosphodiesterase (E), releasing the inhibitory influence of one of the E γ subunits. The activated E begins to hydrolyze cGMP (cG) to GMP. The resulting fall in cytosolic cGMP concentration causes cGMP molecules to dissociate from the ion channel, which now closes. Rod recovery occurs in part due to an increase in cGMP concentration, which is synthesized from GTP by guanylate cyclase (GC). Reproduced with permission from Reference 78.

One limitation of conventional ERG analysis is that the ERG waveforms are formed by a composite of generators and thus are nonspecific in terms of cellular origin. For example, the ERG b-wave contains not only bipolar responses but also contributions from the photoreceptor a-wave and oscillatory potentials from the proximal retinal layers (18). The b-wave also includes a substantial corneal negative scotopic threshold response generated by the proximal retina at low-to-moderate flash intensities (18,28). In most of the studies investigating the role of fatty acids in retinal function, the ERG has typically been measured up to flash intensities sufficient to produce maximal ERG b-wave amplitude (V_{max}). At this flash intensity, the ERG a-wave does not provide an accurate description of the massed hyperpolarization response of the photoreceptors (16).

Analysis of phototransduction. Recent developments in ERG recording and analysis techniques have enabled better isolation of the massed responses from the photoreceptor and bipolar cells. *In vitro* experiments with isolated photoreceptors have enabled the development of a quantitative model describing the G-protein cascade of phototransduction (29). The same quantitative model or slight variants of it (see Eq. 2) have been used successfully to describe the leading edge of the ERG a-wave in response to a high intensity flash that causes a-wave saturation (22,30–32). Figure 6 shows an example of ERG recorded to three different flash intensities (solid lines) and the fit of the model given in Equation 2 to the leading edges of the ERG a-waves (dashed lines). The phototransduction model is given by

$$P3(i, t) \approx \{1 - \exp[-i \cdot S \cdot (t - t_d)^2]\} \cdot R_{\max P3} \quad t > t_d \quad [2]$$

where $P3$ is the voltage of the ERG a-wave (μV), at time t seconds, in response to a flash with a retinal illuminance of i scot Td-sec. The $P3$ term describing the ERG a-wave is so named after Granit's classic analysis, in which the ERG was formed by the addition of two cellular responses, $P2$, a single postreceptoral response and $P3$ the response from the pho-

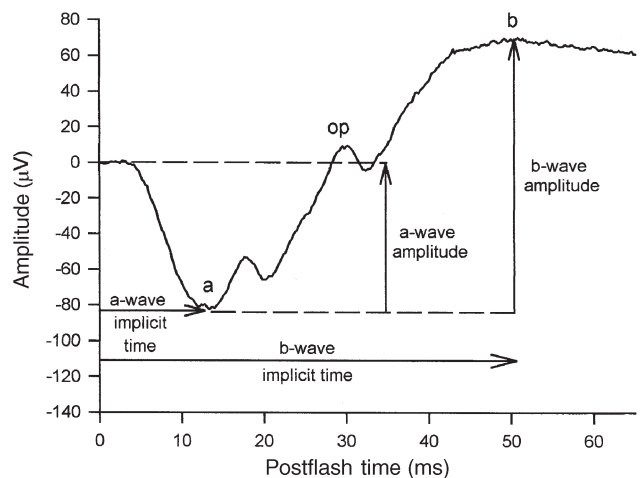


FIG. 3. The electroretinogram (ERG) a-wave represents the hyperpolarization of the massed photoreceptor response, whereas the ERG b-wave represents the depolarization of the rod-bipolar cells. Small oscillatory potentials shown superimposed on the rising b-wave originate from interactions among the amacrine, interplexiform, and ganglion cells. ERG a-wave amplitude is measured from the baseline to the trough of the ERG a-wave, and ERG b-wave amplitude is measured from the trough of the a-wave to the peak of the ERG b-wave. Implicit times are measured from flash onset (time 0) to the trough of the ERG a-wave and to the peak of the ERG b-wave.

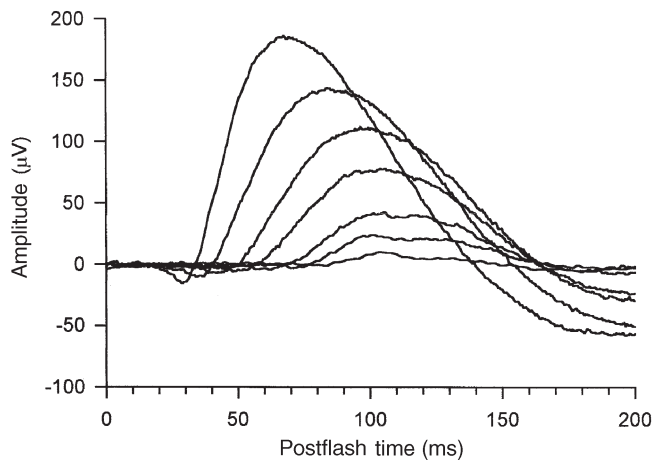


FIG. 4. Variation in ERG b-wave amplitude and implicit time over a 4 log unit range of retinal illuminance. With increasing retinal illuminance (bottom to top), ERG b-wave amplitude increases and implicit time decreases. For abbreviation see Figure 3.

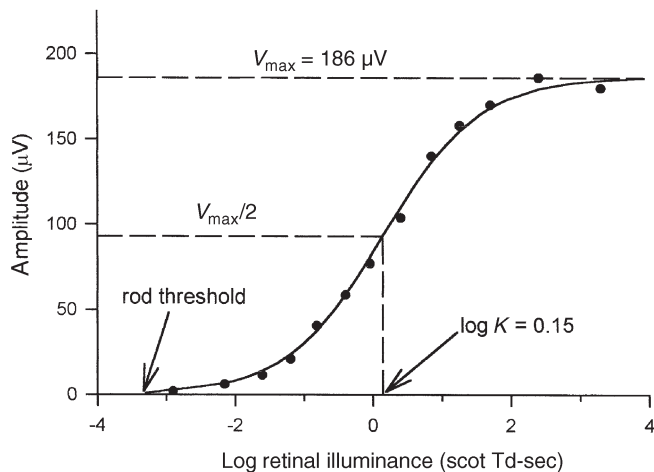


FIG. 5. Variation in ERG b-wave amplitude with retinal illuminance from an adult rhesus monkey. The solid line shows the fit of the Naka-Rushton equation (Eq. 1 in text) to the data. The parameters derived from the fit of the Naka-Rushton equation are as follows: V_{\max} , the maximum amplitude (μV), and K , the intensity that elicits half-maximal response. Rod threshold, defined as the flash intensity at which an ERG b-wave is just detectable, may also be derived from the Naka-Rushton equation. For abbreviation see Figure 3.

toreceptors (33,34). The parameters of the model that are adjusted to provide the best description of the leading edge of the rod isolated ERG a-wave are as follows: S , a sensitivity parameter that scales retinal illuminance [$(\text{scot Td-sec})^{-1} \text{sec}^{-2}$]; t_d , a delay (sec), and $R_{\max P_3}$, the maximum amplitude response (μV) (35). The parameter S has been interpreted to represent the gain of the phototransduction cascade, i.e., it is proportional to the number of cation channels closed per molecule of rhodopsin activated (22,30). Alternatively, S may also be altered by a change in the local rhodopsin density on the disk membrane (22,30). $R_{\max P_3}$ is the change in voltage corre-

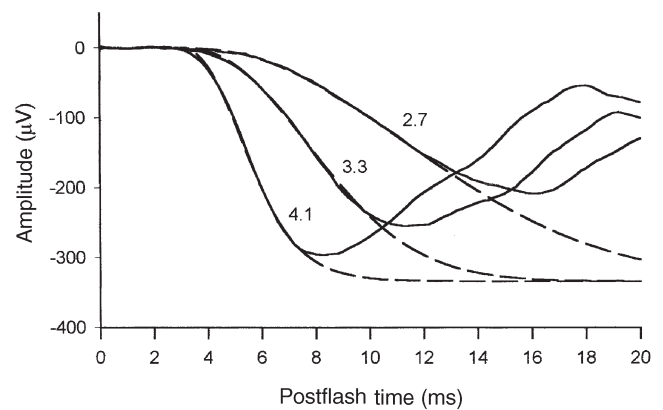


FIG. 6. The P_3 model given by Equation 2 (see main text) provides an excellent fit (dashed lines) to the leading edges of the rod-isolated ERG a-waves (solid lines). The numbers above each ERG a-wave indicate the retinal illuminance in log scot Td-sec used to generate the ERG.

sponding to the maximum number of cation channels that can be closed. A reduction in the number of photoreceptors or shortening in the length of the ROS would cause a proportional reduction in $R_{\max P_3}$ (22,30). The parameter t_d is a non-physiologic delay due to instrumentation filtering and finite duration of the flash. One variation to the model given in Equation 2 is to include a term that accounts for membrane capacitance (32,36). Membrane capacitance becomes an important factor when describing the cone photoreceptor ERG a-wave or the rod ERG a-wave recorded to extremely bright flash intensities (31,32,36). Employing the model given by Equation 2 to describe the ERG a-wave thereby provides an *in vivo* method of quantifying the phototransduction process.

To derive the phototransduction parameters, S , $R_{\max P_3}$, and, t_d Equation 2 is typically fitted simultaneously to multiple ERG a-waves recorded to a series of bright flashes (ensemble fit) (Fig. 6). The highest retinal illuminance used in Figure 6 is ~ 500 times brighter than the illuminance required to produce ERG b-wave saturation, as used in conventional ERG analysis.

Assessment of rod recovery. After light capture, the phototransduction proteins (R^* , G^* , and E^*) are activated, and cytosolic cGMP concentration falls, closing a portion of the cGMP-gated ion channels that are open (Fig. 2). Before the rod can fully respond to subsequent photons of light, the rod must be returned to its dark-adapted resting state. The steps necessary for rod recovery include deactivation of R^* , G^* , and E^* and the return of cGMP concentration to its preflash level. The latter step reopens the same proportion of cGMP-gated ion channels that were closed by the flash. The time course of rod recovery can be assessed using a paired-flash ERG method (35,37). With the paired-flash method, a high intensity “test” flash that forces the rod into saturation is followed by a second “probe” flash at varying interstimulus intervals (Fig. 7). If the probe flash is delivered during the period of rod saturation when all cation channels are closed, there will be no measurable ERG response (Fig. 7, ERG at 6-sec interstimulus in-

terval). Once cation channels begin to reopen, a subsequent probe flash will close all newly opened cation channels, driving the rod back into saturation. The amplitude of the ERG a-wave to the probe flash is proportional to the number of cation channels closed and therefore, the amount of recovery that has occurred since the test flash (35,38). Figure 7 illustrates the recovery of ERG amplitude (thin solid lines) from an adult rhesus monkey at various interstimulus intervals after a bright test flash (5.4 log scot Td-sec). At the end of the recovery experiment, the ERG is recorded in response to a probe flash presented in isolation without a preceding test flash ("Probe only," Fig. 7). The dashed lines in Figure 7 show the fits of the P3 model (Eq. 2) to the leading edges of each ERG a-wave. The maximal response derived at each interstimulus interval (ISI), $R_{\max\text{ISI}}$, is normalized with respect to the maximal response derived from the isolated probe response (IPR), $R_{\max\text{IPR}}$. Figure 8 shows the plot of the normalized responses $R_{\max\text{ISI}}/R_{\max\text{IPR}}$ against log interstimulus interval. The solid line is the best fit of the sum of two exponentials to the data. Also shown are two characteristic parameters derived from the analysis, i.e., T_c , the time the rod remains saturated after the test flash and T_{50} , the time required from T_c to reach 50% of full recovery.

DHA IN THE RETINA

Within the retina, DHA is incorporated primarily into structural glycerophospholipids of the cell membrane lipid bilayer (39). DHA accounts for 8–20% of total retinal fatty acids in humans and 38–92% of total polyunsaturates within the mammalian retina (2,40–45). DHA is particularly concentrated

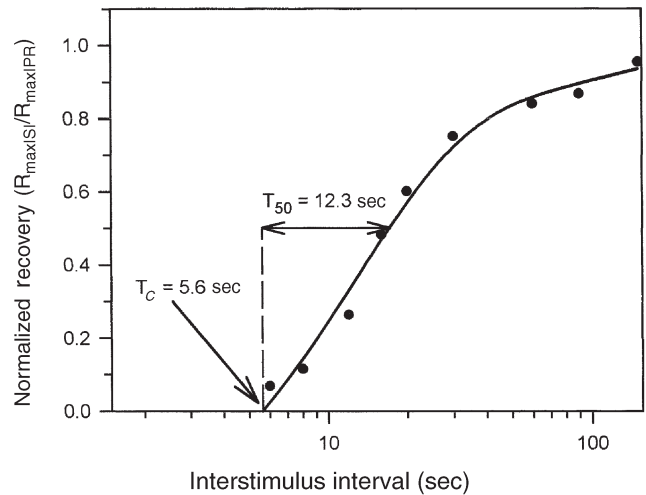


FIG. 8. Normalized ERG a-wave recovery plotted against interstimulus interval. The amplitudes of the probe flash ERG at each interstimulus interval (ISI) ($R_{\max\text{ISI}}$) are normalized with respect to the amplitude of the isolated probe response (IPR) flash ERG recorded at the end of the sequence ($R_{\max\text{IPR}}$). The solid line is the best fit of the sum of two exponentials to the data. Also shown are two characteristic parameters derived from the analysis, T_c and T_{50} . For abbreviation see Figure 3.

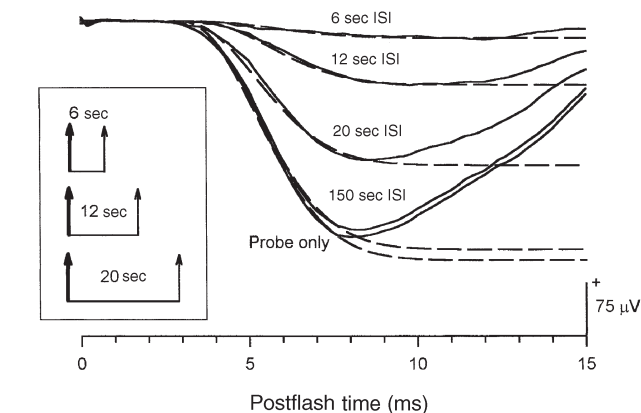


FIG. 7. Recovery of the rod ERG a-wave after a saturating flash. The solid lines show the rod isolated ERG recorded to the second (probe) flash (4.1 log scot Td-sec) at a given interstimulus interval (ISI) after a test flash (5.45 log scot Td-sec). The bottom-most response (probe only) is the ERG recorded to the probe flash presented without a preceding test flash 150 sec after the last double flash pair. The dashed curves show the best fits of Equation 2 to the leading edges of the ERG a-waves. Inset: Graphic representation of the separation between the saturating test flash (thick arrow) followed by the probe flash (thin solid arrow) at a given interstimulus interval. For abbreviation see Figure 3.

within the disk membranes of the ROS where it accounts for up to 30% of total fatty acids and 54% of phosphatidylethanolamine (PE) fatty acids (2,42,46,47). The retina is unique in that it contains phospholipids with polyunsaturates at both the *sn*-1 and *sn*-2 positions (dipolyenes). In the monkey, dipolyenes with long-chain polyunsaturated fatty acids (LC-PUFA) in both the *sn*-1 and *sn*-2 positions constitute 16% of the diacyl ethanolamine phosphoglycerides, and 15% of these have DHA in both positions (48).

LC-PUFA SUPPLEMENTATION IN HUMAN AND NONHUMAN PRIMATES

Birch *et al.* (27) reported an elevation in log *K* and a reduction in V_{\max} at 36 wk postconception (~6 wk postnatal age) in preterm infants fed a corn oil-based formula with a low level (0.5%) of α -linolenic acid (ALA) compared with infants fed a fish oil-supplemented formula [0.35% DHA and 0.65% eicosapentaenoic acid (EPA)]. Analysis of the Naka-Rushton function from these infants also revealed an elevation in rod threshold in the corn oil group, which likely reflects the elevation in log *K*. Infants fed a soybean oil-based diet (2.7% ALA) had parameter values that were in between those of the corn and fish oil diet groups. In a follow-up study of term infants by the same group, only log *K* was elevated at 6 wk postnatal age in infants fed a formula with 1.7% ALA as the sole n-3 fatty acid, compared with infants fed a formula supplemented with LC-PUFA [0.36% DHA, 0.72% arachidonic acid (AA)] (49). In both studies, the early differences noted in the ERG between the diet groups were no longer present at 4 mon of age (cor-

rected age for premature infants). However, in the preterm study, infants in the corn oil group had longer latencies for light-adapted oscillatory potentials at 4 mon corrected age (27).

In another study, term infants were randomized to either a control formula containing 2.1% ALA as the sole n-3 fatty acid or one of two formulas supplemented with LC-PUFA, either 0.12% DHA and 0.43% AA, or solely 0.23% DHA. There were similarly no ERG differences between the diet groups at the sole test age of 4 mon (50).

Owing to limitations in ERG methodology used, results from a fourth study are difficult to interpret. Faldella *et al.* (51) recorded ERG from a skin electrode placed on the bridge of the nose. ERG recorded from this position exhibit high variability, are extremely small, and lack the sensitivity even to distinguish different forms of retinal pathology (52). The failure to dilate the pupil or dark-adapt the infants in this study would have further reduced ERG amplitudes and increased variability of the recordings. Given these limitations, it is difficult to draw any conclusions about the effects on retinal function of the diets used in this study.

The preterm infants in the study of Birch *et al.* (27) were born at 28–33 wk gestation. Over the last trimester of pregnancy, there is a 35% increase in retinal DHA level (40), and infants born prematurely are likely to be more susceptible to any reduction in the availability of DHA for accretion by the retina. This greater susceptibility in infants born prematurely may explain the more marked ERG alterations at 6 wk postnatal age in the preterm infants compared with the term infants. Other differences between the term and premature infant studies, notably the level of dietary ALA used, may also account for the greater ERG alterations in the premature infants. The results from both preterm and term infants suggest that retinal function may be altered by the level of n-3 fatty acids supplied in the diet for at least the first six postnatal weeks.

Owing to the difficulty of recording ERG with a contact lens in older infants and young children, the evaluation of retinal function after varying dietary n-3 fatty acid content has been limited to a maximum of 4 mon postterm in humans. The rhesus monkey provides an ideal animal model of the human for the long-term study of the effect of diet on retinal function. The similarities between retinal structure, function, and development in macaque monkeys (e.g., rhesus) and humans are well described (11,53–56). Additionally, rhesus monkeys, like humans, are capable of desaturating and elongating the n-3 and n-6 essential fatty acids to obtain their respective long-chain polyunsaturates (57–60). Adjustments necessary for comparison of humans and macaque monkeys are the different rates of visual development (1 wk for monkeys is equivalent to ~4 wk in humans) and the greater neural and retinal maturity of the monkey at birth.

In a recent study, infant monkeys were raised for the first six postnatal months on either a formula containing 1.7% ALA as the sole n-3 fatty acid or a diet supplemented with 0.8% DHA and 0.8% AA. At 4 and 13 mon of age, there were no significant differences in rod or cone ERG between the two diet groups (62).

In a separate study, retinal function was assessed in monkeys raised their entire lives on either a diet with 8% ALA as the sole n-3 fatty acid or a diet supplemented with 0.6% DHA and 0.2% AA. The mothers of these monkeys consumed diets identical to those of their offspring throughout pregnancy. There were no significant differences in the ERG between the two groups of monkeys when tested as adults (4–6 yr) (62). However, several alterations were found in the ERG of monkeys fed very low ALA diets, and these are described in the following section.

The results from the two monkey studies suggest that a diet with 1.7–8% ALA as the sole n-3 fatty acid does not adversely affect the long-term development of retinal function in higher primates, compared with a diet containing at least 0.6% DHA. The similarity of the rhesus monkey retina to that of humans, together with the data for human infants at 4 mon, suggests that this finding is likely valid for humans. It has not been tested in humans whether a diet with a level of ALA >1.7% would eliminate the alterations in the ERG noted at 6 wk postnatal age compared with infants fed a LC-PUFA-supplemented diet containing 0.35% DHA.

The combined results from the human and monkey studies suggest that the period of vulnerability of the retina to a low supply of dietary n-3 fatty acids is short. If a lowering of retinal DHA level underlies the ERG alterations reported in the human infants, what are the possible mechanisms that result in this early vulnerability? In both rhesus monkeys and baboons, DHA is readily accreted by the retina from the circulating blood supply during the latter stages of fetal development and during the neonatal period (57–59). The retina also has a sophisticated recycling system that ensures conservation of retinal DHA levels even during periods of prolonged dietary n-3 deficiency (4–6). Both term and preterm human infants are capable of synthesizing some DHA from ALA (63,64). However, the above results suggest that infants, particularly preterm infants, fed formulas with <1.7% ALA may not be able to synthesize sufficient DHA to meet their retinal requirements over the early postnatal weeks. The lack of ERG differences at 4 mon of age suggests that any such limitation is transient.

THE EFFECT OF DHA DEFICIENCY ON RETINAL FUNCTION IN ANIMALS

Rats and guinea pigs. Reductions in conventional ERG a- and b-wave amplitudes have been consistently reported in rats and guinea pigs fed n-3-deficient diets in comparison with control animals fed high ALA, n-3-sufficient diets (46,65–70).

The newer methods of ERG recording and analysis have been used in only a few studies. Weisinger *et al.* (70) reported that phototransduction sensitivity, S , varies as a saturating function of retinal DHA level at 16 wk of age in guinea pigs (Fig. 9, lower graph). In the same guinea pigs, the maximal rod response $R_{\max P_3}$ was reduced by ~0.16 log units when retinal DHA fell below 16% of total fatty acids (Fig. 9, upper graph). Further reductions in retinal DHA did not produce any additional loss in $R_{\max P_3}$. The pattern of variation in S with

retinal DHA level differs from that of $R_{\max P3}$, suggesting that two separate mechanisms may be affected in n-3-deficient guinea pigs. In a subsequent study in rats from the same laboratory, a reduction in retinal DHA from 34.1 to 25.5% of total fatty acids was associated with a 0.28 log unit reduction in both $R_{\max P3}$ and S at 35 wk of age (71).

The mechanisms by which lowering retinal DHA levels causes reductions in ERG amplitudes and phototransduction sensitivity in rats and guinea pigs are not yet fully understood. The rate of ROS disk synthesis (42), the number of photoreceptors (46,72), ROS length (42,72), and the width of the outer nuclear layer (42) remain unaltered in n-3-deficient rats. The number of retinal pigment epithelium (RPE) phagosomes is reduced in n-3-deficient rats (66,73), but such changes seem unlikely to alter ERG components generated by the photoreceptors and bipolar cells within the first 70 msec after flash onset. Alteration in the local concentration of rhodopsin within the ROS would likely affect phototransduction sensitivity (30), and the rate of rhodopsin regeneration after a 100% bleach is slowed in n-3-deficient rats (72). However, slower rhodopsin regeneration is unlikely to have caused the

ERG alterations in n-3-deficient rats and guinea pigs, given that all studies, with the exception of Watanabe *et al.* (66), allowed sufficient time to achieve full dark adaptation. There are conflicting reports as to the effect of altering the level of dietary n-3 fatty acids on absolute rhodopsin content in the retina after complete dark adaptation. Higher levels of rhodopsin have been reported in rats fed either an n-3-deficient diet (72) or a high DHA/EPA fish oil-supplemented diet (74) compared with rats fed a diet containing ALA as the sole n-3 fatty acid. Further experiments are required to determine whether altered rhodopsin levels underlie the sensitivity changes reported in rats and guinea pigs. Higher rhodopsin levels in n-3-deficient rats might be expected to lead to higher rather than lower sensitivity. However, low DHA in the membrane lipid environment of rhodopsin may reduce its photochemical activity and thus lower sensitivity. This possibility is supported by *in vitro* model membrane studies showing lower metarhodopsin II formation in membranes low in DHA (75–77).

Another possibility is that low retinal DHA affects the ERG through changes in ion channels. $R_{\max P3}$ is proportional to the magnitude of the circulating photocurrent, i.e., the number of open cGMP-gated ion channels within the retina (22). The number of cGMP-gated ion channels open at any given time is regulated by intracellular cGMP concentration, which in turn depends on the rates of cGMP hydrolysis and synthesis. A number of the mechanisms involved in determining the rates of cGMP hydrolysis and synthesis are Ca^{2+} dependent (78). On the basis of the results from experiments in monkeys described below, it is speculated that a reduction in retinal DHA may alter the calcium current flowing into the photoreceptor outer segments through the cGMP-gated ion channels. Whether alteration in cytosolic Ca^{2+} concentration underlies the reduction in $R_{\max P3}$ in n-3-deficient rats and guinea pigs remains to be determined.

No significant alterations in ERG a-wave and b-wave implicit times have been reported in n-3-deficient guinea pigs compared with those fed a high ALA diet (68,70). Rats fed a diet with DHA enriched at the *sn*-2 position of triglycerides had a 3.5–5.5% delay in ERG b-wave implicit times compared with rats fed either rat milk or a diet with DHA distributed equally across the *sn*-1, -2, and -3 positions (79). A caveat in interpreting this study is that the delay in ERG implicit times was present for only one of three flash intensities. Absolute retinal fatty acid levels were not significantly different between the two groups fed the experimental diets, but it would be of interest to know whether the experimental diets altered the dipolyene composition of the retinas. The retina is unique in containing a high level of dipolyenes, and these are known to increase the rate of rhodopsin activation (metarhodopsin II formation) compared with monoenes in recombinant membranes (76,77,80). Delays in metarhodopsin II formation or the rate of activation of the phototransduction proteins could slow the ERG response.

Cats. The effects of reducing retinal DHA levels in a single study of cats were quite different from those reported in

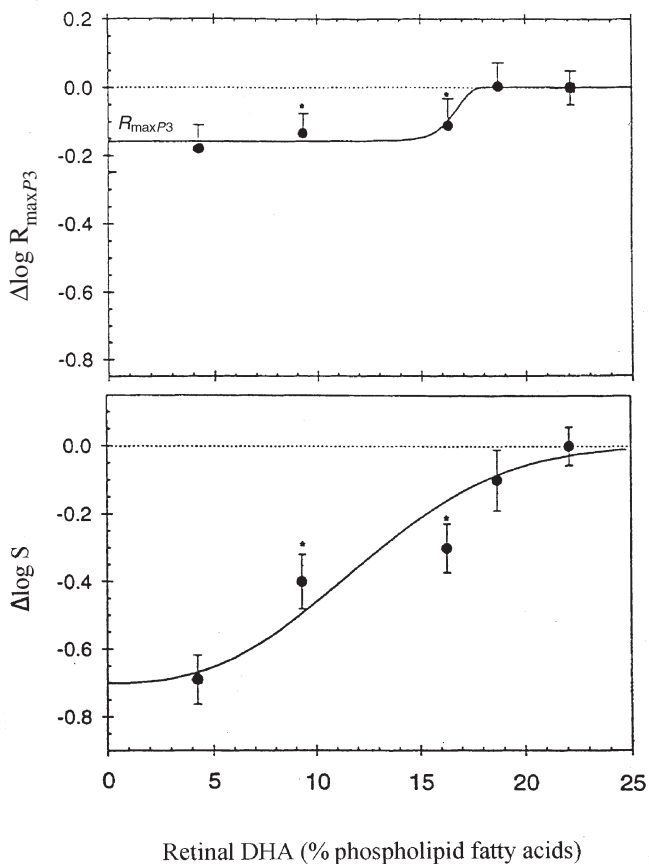


FIG. 9. Variation in S (lower graph) and $R_{\max P3}$ (upper graph) with retinal docosahexaenoic acid (DHA) in 16-wk-old guinea pigs. Values are expressed as the change ($\Delta \log$ value \pm SEM) from control guinea pigs fed a canola oil-based diet. *Significantly different from the canola oil group, $P < 0.05$. Data were fit by a Weibull function to emphasize the transitions. Reproduced with permission from Reference 70.

rats and guinea pigs. In 12-wk-old cats, ERG a-wave implicit times were delayed by 10% in those fed diets with differing levels of ALA (0.2–1.3%) compared with cats fed diets that contained LC-PUFA (>0.3% DHA, >0.5% AA) (81). There were no significant differences in ERG amplitudes between the groups. Delays in ERG b-wave implicit times in this study were reported, but are difficult to interpret because the ERG was recorded to a red flash that elicited a mixed rod/cone response. The mean ERG b-wave implicit time for the LC-PUFA-supplemented cats was 48.6 msec, consistent with the peak of the cone response (23), whereas the mean ERG b-wave implicit time for the ALA cats was 70.7 msec, consistent with the peak of the rod response (23). These results suggest that different ERG b-wave components were measured for the two diet groups, or that the relative amplitudes of these components were altered.

Rhesus monkeys. Neuringer and co-workers (82–85) fed two cohorts of rhesus monkeys diets that contained either 0.3% ALA (Low ALA) or 8% ALA (High ALA) as the sole n-3 fatty acid. The second cohort also included a third dietary group supplemented with LC-PUFA (0.6% DHA, 0.2% AA, and 0.2% EPA). ERG were recorded from the monkeys as infants (3–4 mon), juveniles (1–2 yr), and for the second cohort as young adults (4–6 yr). In the first cohort, Low ALA monkeys had reduced rod and cone ERG a-wave amplitudes as infants compared with the High ALA monkeys (84). This result was not repeated in the second cohort when they were tested at the same age or in either cohort when tested as juveniles or adults (62,84,86). In addition, there was a 5–10% delay in rod and cone ERG b-wave implicit times in the Low ALA monkeys when tested as juveniles and adults compared with monkeys fed the High ALA and LC-PUFA-supplemented diets (62,84,86).

The most marked and consistent alteration in retinal function in monkeys fed the Low ALA diet was a delay in the time required for the rod photoreceptors to recover after a light flash. When moderately intense flashes (2.6 log scot Td-sec) were separated by intervals of 20 sec, ERG amplitudes were not significantly different between the rhesus monkeys fed the Low ALA diet and those fed the High ALA diet. When the interval between flashes was reduced to 3.2 sec, ERG a- and b-wave amplitudes were reduced in both groups of monkeys, but there was a significantly greater reduction in the Low ALA monkeys compared with the High ALA monkeys (83–85). This effect was present in both cohorts of monkeys when tested as infants and juveniles. The reduction in ERG amplitude at short intervals between flashes suggested a delay in recovery of the rod photoreceptors, a conclusion recently confirmed in adult rhesus monkeys by measuring rod recovery with the paired flash method (62,86). The Low ALA monkeys were delayed by ~30% in reaching 50% recovery (T_{50}) compared with the 5% delay in ERG implicit times in the same monkeys (62). There was no effect of diet groups on the duration of complete rod saturation, T_c (62).

Results from *in vitro* experiments using recombinant membranes and isolated cells suggest a number of possible mech-

anisms that could account for the delays in ERG b-wave implicit times and rod recovery in the Low ALA monkeys. Activation of the G-protein cascade involves contact between the activated proteins, R^* , G^* , and E^* as the result of two-dimensional diffusion through the disk membrane lipid bilayer. It has been proposed that the high concentration of DHA and dipolyenes in the disk membrane imparts a number of biophysical properties (77) that should facilitate the diffusion of the phototransduction proteins through the disk membrane. Recent results demonstrate that the diffusion of transducin is faster in model membranes containing DHA at the *sn-2* position than in membranes with oleic acid at the *sn-2* position (87). Thus, slower diffusion of the phototransduction proteins through the lipid bilayer of the disk membrane may account for the small delays in ERG implicit times in n-3-deficient animals. The same principle could also apply to proteins such as rhodopsin kinase and recoverin, which are involved in the deactivation of R^* and thus could help to explain part of the delay in rod recovery as well. However, the delay in rod recovery in the Low ALA adult rhesus monkeys was ~6 times greater than the delay in ERG implicit times, and this discrepancy suggests a separate mechanism in the recovery process that is altered in the Low ALA monkeys. One possibility is that a larger Ca^{2+} current flows through the cGMP-gated cation channels of the Low ALA monkeys. There are numerous processes required for rod recovery, including the deactivation of the phototransduction proteins and the return of cytosolic cGMP concentration to preflash levels. Higher intracellular Ca^{2+} slows the deactivation of metarhodopsin II and the synthesis of cGMP (88); the net effect of both is to slow the rate of rod recovery. DHA as a free fatty acid suppresses voltage-gated L type Na^+ and Ca^{2+} channel currents in isolated neonatal and adult rat cardiomyocytes and in CA1 neurons from the rat hippocampus (89,90). Whether DHA similarly affects the cGMP-gated ion channel of the rod photoreceptor is unknown. A larger transient Ca^{2+} influx through the cGMP-gated ion channels in the Low ALA monkeys could explain the observed delay in rod recovery.

Comparison of ERG results among animal species. The studies in rats, guinea pigs, cats, and rhesus monkeys highlight important species differences with respect to the effect of reducing retinal DHA levels on retinal function. It is unclear why these species should exhibit such contrasting ERG alterations in response to an n-3-deficient diet. In the ERG studies, rats and guinea pigs fed n-3-deficient diets had retinal DHA levels reduced by 30–65% in comparison with n-3-sufficient control animals. In the rhesus monkeys, retinal DHA was reduced by 50% at birth and by 80% at 2 yr of age compared with the High ALA control group. In each of the animal studies described, the fall in retinal DHA was largely compensated for by an increase in retinal 22:5n-6 and, to a lesser extent, 22:4n-6. These comparisons highlight the fact that the n-3-deficient diets used in each species induced similar changes in retinal fatty acids.

The timing of retinal development and accretion of DHA to the retina also appear to be unable to explain the different

ERG results between monkeys and guinea pigs. There is substantial growth and differentiation of retinal cells *in utero* in both monkeys and guinea pigs (53,91), and mothers were fed the same n-3-deficient diets in studies using both species. The structure of the monkey retina is quite different from that of rats and guinea pigs. In higher primates, cones account for ~5% of the total photoreceptors and interact with rods in a complex manner (92). The primate retina also has a macula, a central area containing the pigments, lutein, and zeaxanthin (93). At the center of the macula lies the fovea, a region with very high cone density that enables primates to achieve high visual acuity (94). The retinas of rats and guinea pigs by comparison are specialized for nocturnal vision, are dominated by rod photoreceptors, and have no macula or fovea. Therefore, rats and guinea pigs have excellent sensitivity in the dark but poor visual acuity. It is possible that these differences in retinal structure among species may account for the different effects on retinal function of lowering retinal DHA.

CRITICAL PERIODS FOR ACCRETION OF DHA TO THE RETINA

A number of repletion studies have provided evidence for a "critical period" during retinal development when an inadequate supply of DHA to the retina will result in permanent retinal dysfunction that cannot be normalized even when retinal DHA is returned to normal.

A subset of the monkeys from cohort 1, described previously, was fed the Low ALA diet for 10–22 mon after birth before being switched to a fish oil-based diet containing 9% DHA and 13% EPA (wt% of total fatty acids) (60). After 9 mon of dietary repletion, when DHA levels had increased to above normal, repleted monkeys still had delayed ERG b-wave implicit times and a greater reduction in ERG b-wave amplitude at short interflash intervals compared with control monkeys (84). In this study, repletion was initiated at ages when rhesus monkeys have an adult-like retina (53,95). In one monkey repleted with 1.6% DHA ethyl ester from 4 mon of age, when the retina is not fully developed, the ERG normalized by 2 yr of age (96).

In a study by Armitage *et al.* (71), rats were fed either a safflower oil-based diet with 1% ALA and a LA/ALA ratio of 72:1 or a canola oil-based diet with 8% ALA and a LA/ALA ratio of 2.5:1. At 8 wk of age, half of the rats fed the safflower diet were switched to the canola oil diet for 25 wk. By 33 wk, there were no significant differences in retinal DHA levels between the repleted rats and those fed the canola oil diet. Nevertheless, the repleted rats had a 60% reduction in $R_{\max P3}$ compared with the those fed the canola oil diet. In a similar repletion study using the same diets, no ERG alterations were found in guinea pigs after retinal DHA levels were returned to within 85% of normal after repletion from 5 to 16 wk. In both species, repletion was initiated at an age when the retina has functionally reached adult levels (97).

The above results provide strong support for the existence of a critical period in both monkeys and rats in which DHA

must be accreted to the retina to achieve normal development of retinal function. The length of these critical periods with regard to either age or the stage of retinal development has yet to be determined.

A ROLE FOR DHA IN THE REGENERATION OF RHODOPSIN

Rhodopsin is formed in the disk membrane of the retinal ROS when opsin binds its chromophore, 11-*cis* retinal. The capture of light by 11-*cis* retinal results in its isomerization to all-*trans* retinal and leads to the formation of metarhodopsin II. After deactivation of metarhodopsin II, some of the all-*trans* retinal separates from opsin and is converted to all-*trans* retinol. Regeneration of rhodopsin from these components is a two-step process. First, all-*trans* retinol must be removed from the ROS and transferred to the RPE. Second, a new 11-*cis* retinal molecule manufactured within the RPE must be transferred to the ROS, where it binds opsin to form a new rhodopsin molecule. The mechanism whereby the highly insoluble retinoids, 11-*cis* retinal and all-*trans* retinal, are transferred across the aqueous interphotoreceptor matrix between the RPE and the ROS is known to involve the interphotoreceptor retinal binding proteins (IRBP). The IRBP are the major soluble proteins within the interphotoreceptor matrix, and bind both retinoids and fatty acids (98).

In a single fluorescence study, DHA had the highest affinity for IRBP, twice that of AA and three times that of ALA (99). A subsequent fluorescence study found that DHA hindered the interaction of 11-*cis* retinal at a hydrophilic binding site on IRBP and also facilitated the dissociation of 11-*cis* retinal from this binding site (100). In contrast, DHA did not alter the interaction or dissociation of all-*trans* retinol with IRBP. Preliminary data indicate that AA does not affect the interaction of 11-*cis*-retinal with IRBP (100).

Chen *et al.* (100) reported that the concentration of DHA noncovalently bound to IRBP represented 8.6% of total bound fatty acids in bovine retina. In the same retinas, DHA accounted for 20 and 3.5% of lipids in ROS and RPE, respectively. Thus, there is a DHA concentration gradient between the ROS and RPE. On the basis of the presence of this concentration gradient and the above fluorescence studies, Chen *et al.* (100) proposed the following model for how DHA modulates the transfer of retinoids between the RPE and ROS. When IRBP is located near the RPE, it binds a saturated fatty acid, resulting in high affinity for 11-*cis* retinal at the IRBP hydrophilic binding site. When the IRBP approaches the ROS, DHA will displace the saturated fatty acid from the IRBP because of its higher affinity. The binding of DHA to IRBP will in turn cause a rapid dissociation of 11-*cis* retinal, which moves into the ROS. DHA does not affect the binding affinity of all-*trans* retinol, which moves from the ROS into the hydrophilic binding site on IRBP that was previously occupied by 11-*cis* retinal. When IRBP moves back near the RPE, the process is reversed as DHA is swapped for a saturated fatty acid and the retinoid binding site regains its affinity for 11-*cis* retinal.

There is strong evidence from a single study to suggest that DHA plays an important role in the regeneration of rhodopsin. An 80% reduction in retinal DHA level in n-3-deficient rats was associated with a significantly slower rate of rhodopsin regeneration after a 100% bleach (72). The 11-*cis* retinal necessary for forming rhodopsin is synthesized in the RPE from all-*trans* retinol. The RPE obtains all-*trans* retinol from the choroidal blood supply, and in many mammals, the RPE acts as a secondary store for all-*trans* retinol (9). In rats, the RPE is a relatively weak store for all-*trans* retinol (9), which may make rats more susceptible than other mammals to the effect of lower DHA levels on the rate of rhodopsin regeneration.

SUMMARY AND CONCLUSIONS

Early studies in this field provided conclusive evidence that a reduction in retinal DHA level was associated with altered retinal function as assessed with the ERG. Recent studies have extended these findings to include specific alterations in photoreceptor function in n-3-deficient animals, including slower rod recovery in monkeys and reductions in the maximal response and phototransduction sensitivity in guinea pigs and rats. On the basis of the experiments in n-3-deficient animals, it has been proposed that DHA serves a number of important roles in photoreceptor function, including regulation of retinoid transport between the RPE and ROS and regulation of the Ca²⁺ photocurrent through the cGMP-gated ion channels. It was also proposed that DHA provides the membrane properties that allow the phototransduction proteins to diffuse rapidly through the lipid bilayer of the disk membranes.

The alterations in phototransduction and rod recovery mechanisms in the retina of n-3-deficient animals may be applicable to similar mechanisms in other tissues with high DHA concentration. DHA is also found at high levels within the brain (83,101), which lacks the same efficient mechanism for DHA conservation present within the retina. Several of the mechanisms studied within the photoreceptor are found elsewhere in the body. For example, the phototransduction cascade has a high degree of commonality with the many other signal transduction pathways mediated by G proteins (12,102). Although the ligands may include light, neurotransmitters or hormones, once initiated, the respective G-protein cascades are remarkably similar (12,102). DHA is also found in high concentration within synapses (103,104) where calcium also plays an important role in the modulation of neurotransmitter release (105). The results from ERG experiments with n-3-deficient animals may therefore be relevant for many other neural and physiologic processes. They may also have implications for human infant nutrition despite the lack of ERG alterations beyond 6 wk of age in human infants fed a diet without DHA supplementation.

ACKNOWLEDGMENTS

Dr. Jeffrey was supported by a Ph.D. scholarship from Meadow Lea Foods Australia, and a Flinders University Overseas Research Trip

Award. Dr. Weisinger is supported by a National Health and Medical Research Council (Australia) Part-Time Research Fellowship. Dr. Neuringer was supported by National Institutes of Health grants DK29930 and RR00163 and by The Foundation Fighting Blindness.

REFERENCES

1. Daemen, F.J. (1973) Vertebrate Rod Outer Segment Membranes, *Biochim. Biophys. Acta* 300, 255–288.
2. Fliesler, S.J., and Anderson, R.E. (1983) Chemistry and Metabolism of Lipids in the Vertebrate Retina, *Prog. Lipid Res.* 22, 79–131.
3. Sprecher, H., Luthria, D.L., Mohammed, B.S., and Baykousheva, S.P. (1995) Reevaluation of the Pathways for the Biosynthesis of Polyunsaturated Fatty Acids, *J. Lipid Res.* 36, 2471–2477.
4. Anderson, R.E., O'Brien, P.J., Wiegand, R.D., Koutz, C.A., and Stinson, A.M. (1992) Conservation of Docosahexaenoic Acid in the Retina, *Adv. Exp. Med. Biol.* 318, 285–294.
5. Bazan, N.G., Gordon, W.C., and Rodriguez de Turco, E.B. (1992) Docosahexaenoic Acid Uptake and Metabolism in Photoreceptors: Retinal Conservation by an Efficient Retinal Pigment Epithelial Cell-Mediated Recycling Process, *Adv. Exp. Med. Biol.* 318, 295–306.
6. Stinson, A.M., Wiegand, R.D., and Anderson, R.E. (1991) Recycling of Docosahexaenoic Acid in Rat Retinas During n-3 Fatty Acid Deficiency, *J. Lipid Res.* 32, 2009–2017.
7. Neuringer, M. (1993) The Relationship of Fatty Acid Composition to Function in the Retina and Visual System, in *Lipids, Learning, and the Brain: Fats in Infant Formulas*, (Dobbing, J., ed.) pp. 134–163, Ross Laboratories, Columbus.
8. Tessier-Lavigne, M. (1991) Phototransduction and Information Processing in the Retina, in *Principles of Neural Science*, (Kandel, E.R., and Schwartz, J.H., eds.) pp. 400–418, Elsevier, New York.
9. Rodieck, R.W. (1998) *The First Steps in Seeing*, Sinauer Associates, Sunderland, MA.
10. Weisinger, H.S., Vingrys, A.J., and Sinclair, A.J. (1996) Electrodiagnostic Methods in Vision, Part 2. Origins of the Flash ERG, *Clin. Exp. Optom.* 79, 97–105.
11. Jacobs, G.H. (1996) Primate Photopigments and Primate Color Vision, *Proc. Natl. Acad. Sci. USA* 93, 577–581.
12. Stryer, L. (1986) Cyclic GMP Cascade of Vision, *Annu. Rev. Neurosci.* 9, 87–119.
13. Heckenlively, J.R., and Arden, G.B. (1991) *Principles and Practice of Clinical Electrophysiology of Vision*, Mosby, New York.
14. Kriss, A., Jeffrey, B., and Taylor, D. (1992) The Electroretinogram in Infants and Young Children, *J. Clin. Neurophysiol.* 9, 373–393.
15. Hood, D.C., and Birch, D.G. (1990) The a-Wave of the ERG as a Quantitative Measure of Human Receptor Activity, in *Digest of Topical Meeting on Noninvasive Assessment of the Visual System*, 1990, pp. 66–68, Optical Society of America, Washington.
16. Hood, D.C., and Birch, D.G. (1990) The a-Wave of the Human Electroretinogram and Rod Receptor Function, *Invest. Ophthalmol. Vis. Sci.* 31, 2070–2081.
17. Robson, J.G., and Frishman, L.J. (1995) Response Linearity and Kinetics of the Cat Retina: The Bipolar Cell Component of the Dark-Adapted Electroretinogram, *Vis. Neurosci.* 12, 837–850.
18. Hood, D.C., and Birch, D.G. (1996) Beta Wave of the Scotopic (rod) Electroretinogram as a Measure of the Activity of Human ON-Bipolar Cells, *J. Opt. Soc. Am. A* 13, 623–633.
19. Sieving, P.A., Murayama, K., and Naarendorp, F. (1994) Push-Pull Model of the Primate Photopic Electroretinogram: A Role

- for Hyperpolarizing Neurons in Shaping the b-Wave, *Vis. Neurosci.* 11, 519–532.
20. Heynen, H., Wachtmeister, L., and van Norren, D. (1985) Origin of the Oscillatory Potentials in the Primate Retina, *Vis. Res.* 25, 1365–1373.
 21. Wyszecki, G., and Stiles, W.S. (1982) *Color Science: Concepts and Methods, Quantitative Data and Formulae*, John Wiley & Sons, New York.
 22. Breton, M.E., Schueller, A.W., Lamb, T.D., and Pugh, E.N., Jr. (1994) Analysis of ERG a-Wave Amplification and Kinetics in Terms of the G-Protein Cascade of Phototransduction, *Invest. Ophthalmol. Vis. Sci.* 35, 295–309.
 23. Birch, D.G., and Anderson, J.L. (1992) Standardized Full-Field Electroretinography. Normal Values and Their Variation with Age, *Arch. Ophthalmol.* 110, 1571–1576.
 24. Fulton, A.B., and Rushton, W.A. (1978) The Human Rod ERG: Correlation with Psychophysical Responses in Light and Dark Adaptation, *Vis. Res.* 18, 793–800.
 25. Hood, D.C., and Birch, D.G. (1992) A Computational Model of the Amplitude and Implicit Time of the b-Wave of the Human ERG, *Vis. Neurosci.* 8, 107–126.
 26. Fulton, A.B., and Hansen, R.M. (1988) Scotopic Stimulus/Response Relations of the b-Wave of the Electroretinogram, *Doc. Ophthalmol.* 68, 293–304.
 27. Birch, D.G., Birch, E.E., Hoffman, D.R., and Uauy, R.D. (1992) Retinal Development in Very-Low-Birth-Weight Infants Fed Diets Differing in Omega-3 Fatty Acids, *Invest. Ophthalmol. Vis. Sci.* 33, 2365–2376.
 28. Robson, J.G., and Frishman, L.J. (1996) Photoreceptor and Bipolar Cell Contributions to the Cat Electroretinogram: A Kinetic Model for the Early Part of the Flash Response, *J. Opt. Soc. Am. A* 13, 613–622.
 29. Lamb, T.D., and Pugh, E.N., Jr. (1992) A Quantitative Account of the Activation Steps Involved in Phototransduction in Amphibian Photoreceptors, *J. Physiol.* 449, 719–758.
 30. Hood, D.C., and Birch, D.G. (1994) Rod Phototransduction in Retinitis Pigmentosa: Estimation and Interpretation of Parameters Derived from the Rod a-Wave, *Invest. Ophthalmol. Vis. Sci.* 35, 2948–2961.
 31. Cideciyan, A.V., and Jacobson, S.G. (1996) An Alternative Phototransduction Model for Human Rod and Cone ERG a-Waves: Normal Parameters and Variation with Age, *Vis. Res.* 36, 2609–2621.
 32. Smith, N.P., and Lamb, T.D. (1997) The a-Wave of the Human Electroretinogram Recorded with a Minimally Invasive Technique, *Vis. Res.* 37, 2943–2952.
 33. Granit, R. (1933) The Components of the Retinal Action Potential in Mammals and Their Relation to the Discharge in the Optic Nerve, *J. Physiol.* 77, 207–239.
 34. Granit, R. (1947) *Sensory Mechanism of the Retina*, Oxford University Press, London.
 35. Birch, D.G., Hood, D.C., Nusinowitz, S., and Pepperberg, D.R. (1995) Abnormal Activation and Inactivation Mechanisms of Rod Transduction in Patients with Autosomal Dominant Retinitis Pigmentosa and the pro-23-his Mutation, *Invest. Ophthalmol. Vis. Sci.* 36, 1603–1614.
 36. Hood, D.C., and Birch, D.G. (1993) Human Cone Receptor Activity: The Leading Edge of the a-Wave and Models of Receptor Activity, *Vis. Neurosci.* 10, 857–871.
 37. Pepperberg, D.R., Birch, D.G., and Hood, D.C. (1997) Photoreponses of Human Rods *in vivo* Derived from Paired-Flash Electroretinograms, *Vis. Neurosci.* 14, 73–82.
 38. Pepperberg, D.R., Birch, D.G., Hofmann, K.P., and Hood, D.C. (1996) Recovery Kinetics of Human Rod Phototransduction Inferred from the Two-Branched Alpha-Wave Saturation Function, *J. Opt. Soc. Am. A* 13, 586–600.
 39. Salem, N., Jr., Kim, H.Y., and Yergey, J.A. (1986) Docosa-hexaenoic Acid: Membrane Function and Metabolism, in *Health Effects of Polyunsaturated Fatty Acids in Seafoods*, (Simopoulos, A.P., Kifer, R.R., and Martin, R.E., eds.) pp. 263–317, Academic Press, Orlando.
 40. Martinez, M., Ballabriga, A., and Gil-Gibernau, J.J. (1988) Lipids of the Developing Human Retina: I. Total Fatty Acids, Plasmalogens, and Fatty Acid Composition of Ethanolamine and Choline Phosphoglycerides, *J. Neurosci. Res.* 20, 484–490.
 41. Hrboticky, N., MacKinnon, M.J., and Innis, S.M. (1991) Retina Fatty Acid Composition of Piglets Fed from Birth with a Linoleic Acid-Rich Vegetable-Oil Formula for Infants, *Am. J. Clin. Nutr.* 53, 483–490.
 42. Wiegand, R.D., Koutz, C.A., Stinson, A.M., and Anderson, R.E. (1991) Conservation of Docosahexaenoic Acid in Rod Outer Segments of Rat Retina During n-3 and n-6 Fatty Acid Deficiency, *J. Neurochem.* 57, 1690–1699.
 43. Gülcan, H.G., Alvarez, R.A., Maude, M.B., and Anderson, R.E. (1993) Lipids of Human Retina, Retinal Pigment Epithelium, and Bruch's Membrane/Choroid: Comparison of Macular and Peripheral Regions, *Invest. Ophthalmol. Vis. Sci.* 34, 3187–3193.
 44. Makrides, M., Neumann, M.A., Byard, R.W., Simmer, K., and Gibson, R.A. (1994) Fatty Acid Composition of Brain, Retina, and Erythrocytes in Breast- and Formula-Fed Infants, *Am. J. Clin. Nutr.* 60, 189–194.
 45. Salem, N., Jr. (1989) Omega-3 Fatty Acids: Molecular and Biochemical Aspects, in *New Protective Roles for Selected Nutrients*, pp. 109–228, Alan R. Liss, New York.
 46. Benolken, R.M., Anderson, R.E., and Wheeler, T.G. (1973) Membrane Fatty Acids Associated with the Electrical Response in Visual Excitation, *Science* 182, 1253–1254.
 47. Bazan, H.E.P., Bazan, N.G., Feeney-Burns, L., and Berman, E.R. (1990) Lipids in Human Lipofuscin-Enriched Subcellular Fractions of Two Age Populations: Comparison with Rod Outer Segments and Neural Retina, *Invest. Ophthalmol. Vis. Sci.* 31, 1433–1443.
 48. Lin, D.S., Anderson, G.J., Connor, W.E., and Neuringer, M. (1994) Effect of Dietary n-3 Fatty Acids upon the Phospholipid Molecular Species of the Monkey Retina, *Invest. Ophthalmol. Vis. Sci.* 35, 794–803.
 49. Locke, K.G., Birch, E.E., Hoffman, D.R., Uauy, R., and Birch, D.G. (1998) Effect of Dietary DHA on Retinal Development in Healthy Full-Term Infants, *Invest. Ophthalmol. Vis. Sci.* 39, S829 (abstr.).
 50. Neuringer, M., Fitzgerald, K.M., Weleber, R.G., Murphey, W.H., Giambrone, S.A., Cibis, G.W., and Arends, J. (1995) Electroretinograms in Four-Month-Old Full term Human Infants Fed Diets Differing in Long-Chain n-3 and n-6 Fatty Acids, *Invest. Ophthalmol. Vis. Sci.* 36, S48 (abstr.).
 51. Faldella, G., Govoni, M., Alessandroni, R., Marchiani, E., Salvioli, G.P., Biagi, P.L., and Spanò, C. (1996) Visual Evoked Potentials and Dietary Long Chain Polyunsaturated Fatty Acids in Preterm Infants, *Arch. Dis. Child Fetal Neonatal Ed.* 75, F108–F112.
 52. Lambert, S.R., Kriss, A., Taylor, D., Coffey, R., and Pembrey, M. (1989) Follow-up and Diagnostic Reappraisal of 75 Patients with Leber's Congenital Amaurosis, *Am. J. Ophthalmol.* 107, 624–631.
 53. Hendrickson, A.E. (1993) Morphological Development of the Primate Retina, in *Early Visual Development: Normal and Abnormal*, (Simons, K., ed.) pp. 287–295, Oxford University Press, New York.
 54. Blough, D.S., and Schrier, A.M. (1963) Scotopic Spectral Sensitivity in the Monkey, *Science* 139, 493–494.
 55. Harwerth, R.S., and Smith, E.L. (1985) Rhesus Monkey as a Model for Normal Vision of Humans, *Am. J. Optom. Physiol. Opt.* 62, 633–641.
 56. Fulton, A., Hansen, R.M., Dorn, E., and Hendrickson, A.

- (1996) Development of Primate Rod Structure and Function, in *Infant Vision*, (Vital-Durand, F., Atkinson, J., and Braddick, O.J., eds.) pp. 33–49, Oxford University Press, New York.
57. Sheaff Greiner, R.C., Zhang, Q., Goodman, K.J., Giussani, D.A., Nathanielsz, P.W., and Brenna, J.T. (1996) Linoleate, Alpha-Linolenate, and Docosahexaenoate Recycling into Saturated and Monounsaturated Fatty Acids Is a Major Pathway in Pregnant or Lactating Adults and Fetal or Infant Rhesus Monkeys, *J. Lipid Res.* 37, 2675–2686.
 58. Su, H.M., Bernardo, L., Mirmiran, M., Ma, X.H., Corso, T.N., Nathanielsz, P.W., and Brenna, J.T. (1999) Bioequivalence of Dietary Alpha-Linolenic and Docosahexaenoic Acids as Sources of Docosahexaenoate Accretion in Brain and Associated Organs of Neonatal Baboons, *Pediatr. Res.* 45, 87–93.
 59. Sheaff Greiner, R.C., Winter, J., Nathanielsz, P.W., and Brenna, J.T. (1997) Brain Docosahexaenoate Accretion in Fetal Baboons: Bioequivalence of Dietary Alpha-Linolenic and Docosahexaenoic Acids, *Pediatr. Res.* 42, 826–834.
 60. Connor, W.E., Neuringer, M., and Lin, D.S. (1990) Dietary Effects on Brain Fatty Acid Composition: The Reversibility of n-3 Fatty Acid Deficiency and Turnover of Docosahexaenoic Acid in the Brain, Erythrocytes, and Plasma of Rhesus Monkeys, *J. Lipid Res.* 31, 237–247.
 61. Boothe, R.G., Dobson, V., and Teller, D.Y. (1985) Postnatal Development of Vision in Human and Nonhuman Primates, *Annu. Rev. Neurosci.* 8, 495–545.
 62. Jeffrey, B.G. (2000) The Role of Docosahexaenoic Acid in Retinal Function of the Rhesus Monkey (*Macaca mulatta*), Ph.D. Thesis, The Flinders University of South Australia, Adelaide, Australia, pp. 126–186.
 63. Carnielli, V.P., Wattimena, D.J.L., Luijendijk, I.H.T., Boerlage, A., Degenhart, H.J., and Sauer, P.J.J. (1996) The Very Low Birth Weight Premature Infant Is Capable of Synthesizing Arachidonic and Docosahexaenoic Acids from Linoleic and Linolenic Acids, *Pediatr. Res.* 40, 169–174.
 64. Salem, N., Jr., Wegher, B., Mena, P., and Uauy, R. (1996) Arachidonic and Docosahexaenoic Acids Are Biosynthesized from Their 18-Carbon Precursors in Human Infants. *Proc. Natl. Acad. Sci. USA* 93, 49–54.
 65. Wheeler, T.G., Benolken, R.M., and Anderson, R.E. (1975) Visual Membranes: Specificity of Fatty Acid Precursors for the Electrical Response to Illumination, *Science* 188, 1312–1314.
 66. Watanabe, I., Kato, M., Aonuma, H., Hashimoto, A., Naito, Y., Moriuchi, A., and Okuyama, H. (1987) Effect of Dietary Alpha-Linolenate/Linoleate Balance on the Lipid Composition and Electroretinographic Responses in Rats, *Adv. Biosci.* 62, 563–570.
 67. Bourre, J.-M., Francois, M., Youyou, A., Dumont, O., Piciotti, M., Pascal, G., and Durand, G. (1989) The Effects of Dietary α -Linolenic Acid on the Composition of Nerve Membranes, Enzymatic Activity, Amplitude of Electrophysiological Parameters, Resistance to Poisons and Performance of Learning Tasks in Rats, *J. Nutr.* 119, 1880–1892.
 68. Weisinger, H.S., Vingrys, A.J., and Sinclair, A.J. (1996) Effect of Dietary n-3 Deficiency on the Electroretinogram in the Guinea Pig, *Ann. Nutr. Metab.* 40, 91–98.
 69. Weisinger, H.S., Vingrys, A.J., and Sinclair, A.J. (1995) Dietary Manipulation of Long-Chain Polyunsaturated Fatty Acids in the Retina and Brain of Guinea Pigs, *Lipids* 30, 471–473.
 70. Weisinger, H.S., Vingrys, A.J., Bui, B.V., and Sinclair, A.J. (1999) Effects of Dietary n-3 Fatty Acid Deficiency and Repletion in the Guinea Pig Retina, *Invest. Ophthalmol. Vis. Sci.* 40, 327–338.
 71. Armitage, J.A., Weisinger, H.S., Vingrys, A.J., and Sinclair, A.J. (2000) Perinatal Omega-3 Fatty Acid Deficiency Alters ERG in Adult Rats Irrespective of Tissue Fatty Acid Content, *Invest. Ophthalmol. Vis. Sci.* 41, S245 (abstr.).
 72. Bush, R.A., Malnoe, A., Reme, C.E., and Williams, T.P. (1994) Dietary Deficiency of n-3 Fatty Acids Alters Rhodopsin Content and Function in the Rat Retina, *Invest. Ophthalmol. Vis. Sci.* 35, 91–100.
 73. Bush, R.A., Reme, C.E., and Malnoe, A. (1991) Light Damage in the Rat Retina: The Effect of Dietary Deprivation of n-3 Fatty Acids on Acute Structural Alterations, *Exp. Eye Res.* 53, 741–752.
 74. Reme, C.E., Malnoe, A., Jung, H.H., Wei, J.Q., and Munz, K. (1994) Effect of Dietary Fish Oil on Acute Light Induced Photoreceptor Damage in the Rat Retina, *Invest. Ophthalmol. Vis. Sci.* 35, 78–90.
 75. Wiedmann, T.S., Pates, R.D., Beach, J.M., Salmon, A., and Brown, M.F. (1988) Lipid-Protein Interactions Mediate the Photochemical Function of Rhodopsin, *Biochemistry* 27, 6469–6474.
 76. Brown, M.F. (1994) Modulation of Rhodopsin Function by Properties of the Membrane Bilayer, *Chem. Phys. Lipids* 73, 159–180.
 77. Litman, B.J., and Mitchell, D.C. (1996) A Role for Phospholipid Polyunsaturation in Modulating Membrane Protein Function, *Lipids* 31 (Suppl.), S193–S197.
 78. Pugh, E.N., Jr., Nikonov, S., and Lamb, T.D. (1999) Molecular Mechanisms of Vertebrate Photoreceptor Light Adaptation, *Curr. Opin. Neurobiol.* 9, 410–418.
 79. Christensen, M.M., Lund, S.P., Simonsen, L., Hass, U., Simonsen, S.E., and Høy, C.-E. (1998) Dietary Structured Triacylglycerols Containing Docosahexaenoic Acid Given from Birth Affect Visual and Auditory Performance and Tissue Fatty Acid Profiles in Rats, *J. Nutr.* 128, 1011–1017.
 80. Mitchell, D.C., Straume, M., and Litman, B.J. (1992) Role of *sn*-1-Saturated, *sn*-2-Polyunsaturated Phospholipids in Control of Membrane Receptor Conformational Equilibrium: Effects of Cholesterol and Acyl Chain Unsaturation on the Metarhodopsin I in Equilibrium with Metarhodopsin II Equilibrium, *Biochemistry* 31, 662–670.
 81. Pawlosky, R.J., Denkins, Y., Ward, G., and Salem, N., Jr. (1997) Retinal and Brain Accretion of Long-Chain Polyunsaturated Fatty Acids in Developing Felines: The Effects of Corn Oil-Based Maternal Diets, *Am. J. Clin. Nutr.* 65, 465–472.
 82. Neuringer, M., Connor, W.E., Van Petten, C., and Barstad, L. (1984) Dietary Omega-3 Fatty Acid Deficiency and Visual Loss in Infant Rhesus Monkeys, *J. Clin. Investig.* 73, 272–276.
 83. Neuringer, M., Connor, W.E., Lin, D.S., Barstad, L., and Luck, S. (1986) Biochemical and Functional Effects of Prenatal and Postnatal Omega-3 Fatty Acid Deficiency on Retina and Brain in Rhesus Monkeys, *Proc. Natl. Acad. Sci. USA* 83, 4021–4025.
 84. Neuringer, M., Connor, W.E., Lin, D.S., Anderson, G.J., and Barstad, L. (1991) Dietary Omega-3 Fatty Acids: Effects on Retinal Lipid Composition and Function in Primates, in *Retinal Degenerations*, (Anderson, R.E., Hollyfield, J.G., and La Vail, M.M., eds.) pp. 1–13, CRC Press, New York.
 85. Neuringer, M., Connor, W.E., Anderson, G.J., and Teemer, C.D. (1997) Effects of Dietary Linolenic Acid (18:3n-3) and DHA (22:6n-3) on Electroretinogram Post-Flash Recovery in Rhesus Monkey Infants, *Investig. Ophthalmol. Vis. Sci.* S747 (abstr.)
 86. Neuringer, M., Jeffrey, B.G., and Gibson, R.A. (2000) n-3 Fatty Acid Deficiency Alters Rod Phototransduction and Recovery, *Invest. Ophthalmol. Vis. Sci.* 41, S493 (abstr.).
 87. Mitchell, D.C., Niu, S.L., and Litman, B.J. (2001) Optimization of Receptor-G Protein Coupling by Bilayer Lipid Composition I: Kinetics of Rhodopsin-Transducin Binding, *J. Biol. Chem.*, in press.
 88. Koutalos, Y., and Yau, K.W. (1996) Regulation of Sensitivity in Vertebrate Rod Photoreceptors by Calcium, *Trends Neurosci.* 19, 73–81.
 89. Vreugdenhil, M., Bruehl, C., Voskuyl, R.A., Kang, J., Leaf, A.,

- and Wadman, W.J. (1996) Polyunsaturated Fatty Acids Modulate Sodium and Calcium Currents in CA1 Neurons, *Proc. Natl. Acad. Sci. USA* 93, 12559–12563.
90. Leaf, A. (1995) Omega-3 Fatty Acids and Prevention of Ventricular Fibrillation, *Prostaglandins Leukotrienes Essent. Fatty Acids* 52, 197–198.
91. Huang, J., Wyse, J.P., and Spira, A.W. (1990) Ontogenesis of the Electroretinogram in a Precocial Mammal, the Guinea Pig (*Cavia porcellus*), *J. Comp. Biochem. Physiol.* 95A, 149–155.
92. Wikler, K.C., Williams, R.W., and Rakic, P. (1990) Photoreceptor Mosaic: Number and Distribution of Rods and Cones in the Rhesus Monkey Retina, *J. Comp. Neurol.* 297, 499–508.
93. Bone, B.A., Landrum, J.T., Hime, G.W., Cains, A., and Zamor, J. (1993) Stereochemistry of the Human Macular Carotenoids, *Invest. Ophthalmol. Vis. Sci.* 34, 2033–2040.
94. Wikler, K.C., and Rakic, P. (1990) Distribution of Photoreceptor Subtypes in the Retina of Diurnal and Nocturnal Primates, *J. Neurosci.* 10, 3390–3401.
95. Dorn, E.M., Hendrickson, L., and Hendrickson, A.E. (1995) The Appearance of Rod Opsin During Monkey Retinal Development, *Invest. Ophthalmol. Vis. Sci.* 36, 2634–2651.
96. Neuringer, M., and Connor, W.E. (1990) Supplementation with Docosahexaenoic Acid (22:6 ω -3) Fails to Correct Electroretinogram Abnormalities Produced by Omega-3 Fatty Acid Deficiency in Rhesus Monkeys, *Invest. Ophthalmol. Vis. Sci.* 31, 426 (abstr.).
97. Bui, B.V., and Vingrys, A.J. (1999) Postnatal Development of Receptor Responses in Pigmented and Albino Guinea Pigs (*Cavia porcellus*), *Invest. Ophthalmol. Vis. Sci.* 40, S22 (abstr.).
98. Bazan, N.G., Reddy, T.S., Redmond, T.M., Wiggert, B., and Chader, G.J. (1985) Endogenous Fatty Acids Are Covalently and Noncovalently Bound to Interphotoreceptor Retinoid-Binding Protein in the Monkey Retina, *J. Biol. Chem.* 260, 13677–13680.
99. Chen, Y., Saari, J.C., and Noy, N. (1993) Interactions of all-trans-Retinol and Long-Chain Fatty Acids with Interphotoreceptor Retinoid-Binding Protein, *Biochemistry* 32, 11311–11318.
100. Chen, Y., Houghton, L.A., Brenna, J.T., and Noy, N. (1996) Docosahexaenoic Acid Modulates the Interactions of the Interphotoreceptor Retinoid-Binding Protein with 11-cis-Retinal, *J. Biol. Chem.* 271, 20507–20515.
101. Farquharson, J., Jamieson, E.C., Abbasi, K.A., Patrick, W.J.A., Logan, R.W., and Cockburn, F. (1995) Effect of Diet on the Fatty Acid Composition of the Major Phospholipids of Infant Cerebral Cortex, *Arch. Dis. Child.* 72, 198–203.
102. Yau, K.W. (1994) Phototransduction Mechanism in Retinal Rods and Cones. The Friedenwald Lecture, *Invest. Ophthalmol. Vis. Sci.* 5, 9–32.
103. Cotman, C., Blank, M.L., Moehl, A., and Snyder, F. (1969) Lipid Composition of Synaptic Plasma Membranes Isolated from Rat Brain by Zonal Centrifugation, *Biochemistry* 8, 4606–4612.
104. Sun, G.Y., and Sun, Y. (1972) Phospholipids and Acyl Groups of Synaptosomal and Myelin Membranes Isolated from the Cerebral Cortex of Squirrel Monkey (*Saimiri sciureus*), *Biochim. Biophys. Acta* 280, 306–315.
105. Kandel, E.R., and Schwartz, J.H. (1991) *Principles of Neural Science*, Elsevier, New York.

[Received October 2, 2000; accepted June 20, 2001]